Temperature dependence of continuum and time resolved photoluminescence of germanium nanostructures

M Ardyanian and S A Ketabi

School of Physics, Damghan University, Damghan, Iran
E-mail: ardyanian@du.ac.ir

Abstract

Germanium nanostructures were generated in the post annealed germanium oxide thin films. Visible and near infrared photoluminescence bands were observed in the samples annealed at 350°C and 400°C, respectively. These different luminescence ranges are attributed to the presence of the defects in oxide matrix and quantum confinement effect in the germanium nanostructures, respectively. Decay time and temperature dependence of the luminescence for different bands were investigated, which confirmed our idea about the origin of the luminescence.

Keywords: photoluminescence, nanostructures, germanium, temperature dependence

1. Introduction

Silicon (Si) and germanium (Ge) nanostructures have attracted much attention in the last decade because of their strong potential for optoelectronic applications. Indeed for nanostructures sizes lower than the exciton Bohr radius the confinement of carriers leads to a strong enhancement of the radiative transition and increase of the emitted photons energy. Silicon nanocrystals can be obtained in sub-stoichiometric SiO_x films prepared by Si implantation in SiO_2 [1], sputtering [2] or evaporation [3]. In such silicon sub-oxides, the silicon clusters are generated by post annealing which is involved in the demixtion of the SiO_x film following the reaction,

$$2SiO_x \Rightarrow xSiO_2 + (1-x)Si \qquad (1)$$

Such studies have also been performed to follow the formation of Ge nanocrystals during annealing treatments in $SiGeO_x$ alloys or in GeO_x films prepared by magnetron sputtering [4], but there has been very little work done on the photoluminescence (PL) properties of the Ge nanostructures.

Recently, we have reported on a structural study of GeO_x thin films prepared by evaporation of GeO_2 grains [5]. It was shown that annealing treatments enables us to obtain Ge nanocrystals in a GeO_2 matrix. The PL properties were correlated to the evolution of the structure, in particular to the growth of the nanocrystals, in this manuscript; we interpret the origin of the

observed PL bands corresponding to different annealing temperatures by studying the time resolved PL technique and temperature dependence of intensity and decay time. GeO_2 was evaporated in a high-vacuum chamber from an electron beam gun. The base pressure was 10^{-8} Torr. The pressure during the evaporation increased until 3×10^{-6} Torr. The silicon and silica substrates were maintained at 100°C. The deposition rate of 0.1 *nm/s* was controlled by a quartz microbalance. The layer thickness was 200 nm. After deposition, the films were annealed in a high-vacuum quartz tube with a tubular oven. The heating rate was 10 °C/min. When the annealing temperature *Ta* was reached, this oven was pushed away and the films cooled naturally.

Continuum PL excitation was performed using a He/Cd laser emitting at 325 nm with a 15 *mW* power on the circular surface of 2 *mm* diameter. Optical emission was analyzed by a monochromator equipped with a 600 grooves/mm grating and by a near infrared photo-multiplier tube cooled at 190 K. The detector was an InP/InGaAs photomultiplier cooled at 190K. More sensible set up was utilized for temperature dependence of visible PL; the excitation was effectuated by 313nm UV ray of a mercury vapor tube; the signal was analyzed by a grating monochromator, optimized in visible range and detected by Charge Coupled Device (CCD) camera maintained at 140K.
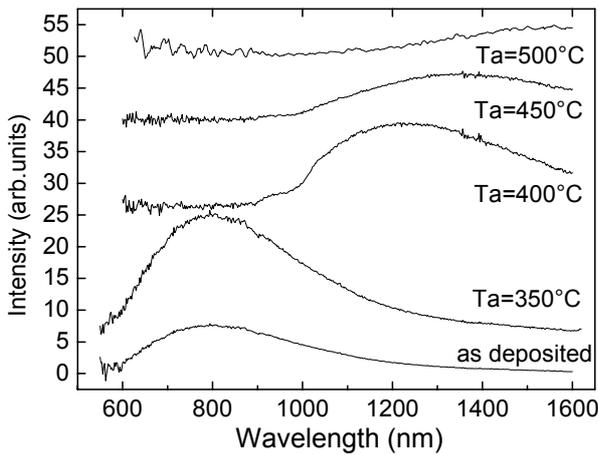
The time resolved photoluminescence excitation at

Figure 1. Photoluminescence Spectra of GeO_x thin films at 77 K for different annealing temperatures (T_a).

355 nm was performed using a frequency trippled YAG:Nd^{3+} laser with an energy of 100 μJ/pulse and repetition rate of 10 Hz. resolution of the system is around 10 ns. The response of the detection system was precisely calibrated with a tungsten wire calibration source. For obtaining the best signal of PL measurements, the films were maintained in a cryostat at 77 K.

2. Results and discussion
2.1. Continuum PL
PL experiments were performed in visible and near IR range (600-1600 nm). The samples were placed in a cryostat and measurements were realized at 77 K for obtaining the best PL signal. In ambient temperature no signal was observed. PL spectra of GeO_x thin films are represented in figure 1. There are different luminescence bands for different annealing temperatures. For annealing up to T_a=350°C the samples present a wide band centered at 800 *nm*. At T_a=400°C the visible bands disappear and a new wide contribution appears about 1200 *nm*. This band shifts to higher wavelengths for higher annealing temperatures up to 500°C. For higher annealing temperatures photoluminescence disappears. We try now to interpret the different contributions of luminescence by the realized experiences.

2.1.1. Visible band at 800 nm
Photoluminescence in visible range was reported in the literature and attributed to different origins. Skuja *et al.* [6] proposed an origin related to oxide matrix for visible PL in the oxide germanium thin films. Also in the SiO_2 thin films implanted with germanium [7] a contribution at 800 nm was attributed to interface states between the Ge nanocrystals and oxide matrix.

In the case of our samples, results of chemical structure study by Fourier transform infrared absorption spectroscopy (FTIR) [5] show that for annealing up to 400 °C the samples have the sub-stoichiometric structure, hence these group of samples probably possess the dangling bands defects of oxygen or germanium.

For annealing temperatures, more than 400°C, the structure of thin films evolved because of appearance of pure Ge in the matrix whose composition is near to GeO_2. It is legal to think that numerous defects related to oxygen or Ge disappear due to thermal annealing. It is known that the thermal treatments lead to suppressing the defects in the thin films; As a consequence of behavior of this visible band, as a function of annealing temperature, we attribute the band centered at 800 nm to the recombination of excitons through the radiative defects in the thin films. We verified our interpretation concerning the origin of visible band by suppressing the dangling band defects; samples ($T_a \leq$ 350 °C) were bombarded under hydrogen plasma and visible part of PL band completely disappeared [8]; this confirms our demonstration, because after suppressing the dangling band defects, the origin of visible luminescence is suppressed and visible PL disappears, too.

2.1.2. Band around 1200 nm
For $T_a \geq$ 400 °C new bands about 1200 nm are observed (figure 1), while the visible PL band centered at 800 nm disappear, for $T_a \leq$ 500 °C this new band shifts toward lower energies and its intensity decreases. This type of evolution was similarly observed in sub-stoichiometric silicon oxide thin films [9], in which the origin of PL is in Si clusters generated due to annealing samples and following reaction,

$$2SiO_x \Rightarrow xSiO_2 + (1-x)Si . \qquad (2)$$
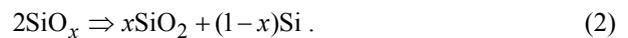
Takeoka *et al.* reported the NIR luminescence band in the Ge doped SiO_2 matrix and attributed it to germanium nanocrystals [10]. In the case of GeO_x thin films, the results of FTIR spectroscopy show the oxygen enrichment of oxide phase toward GeO_2 composition. While Raman spectroscopy results and Transmission electron microscopy [5] describe the appearance of the new phase of pure amorphous Ge for $T_a \geq$ 450 °C related to demixtion of GeO_x following reaction,

$$2GeO_x \Rightarrow xGeO_2 + (1-x)Ge . \qquad (3)$$

Hence the PL band around 1200 nm could be attributed to appearance of pure amorphous Ge in the structure of germanium oxide. The energy of the luminescence peak about 1eV (corresponding to 1200 nm) could be explained by confinement of the carriers in the Ge grains. Redshift of the PL energy and decreasing of PL peak intensity in annealed samples at higher temperatures is in accordance with our interpretation, because annealing implies to grow the Ge grains and diminish the confinement effect. For $T_a \geq$ 550 °C, confinement effect is lost in grand grains and PL disappears. For confirmation of our interpretation, these samples ($T_a \geq$ 400 °C) were bombarded by hydrogen plasma too, but no considerable change was observed in hydrogen bombarded samples [8]. This confirms that the origin of PL bands in visible and near IR bands are completely different.
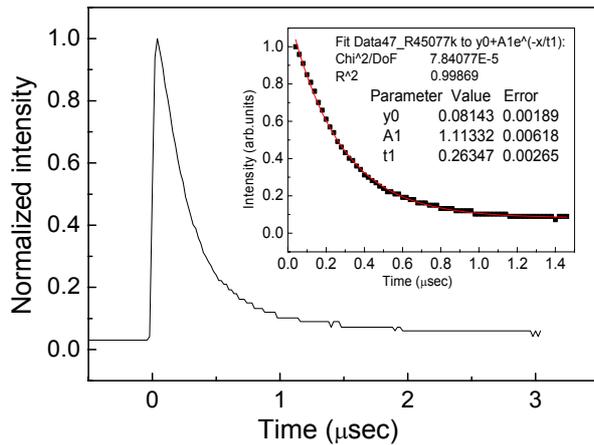
Figure 2. Time resolved PL curve of GeO$_x$ thin films annealed at 450°C which measured at 1350 nm. The measurement temperature was 77K. Inset shows the details of fit calculations based on Chi square test.

Figure 3. (Color online) Photoluminescence Spectra of germanium oxide thin film annealed at 350°C as a function of measurement temperature excited by 313 nm UV Mercury tube. Inset illustrates the sample excited by He-Cd laser.

2.2. Time resolved Photoluminescence
2.2.1. Decay time at 800 nm
Time resolved photoluminescence at 800 nm for as deposited samples and annealed at temperatures less than 400 °C couldn't be measured, because its lifetime is shorter than resolution of our set up (10 ns). This order of magnitude is coherent with the luminescence of defects.

2.2.2. Decay time at 1350 nm
The PL decay curve of the samples annealed at 450°C for the λ=1350 nm (figure 2), is well fitted with exponential decay function $I = I_0 \exp\left(-t / \tau\right)$ with decay time (life time) equal to τ= 270 ns. This value is in the order of magnitude predicted by calculations of Niquet et al. [11], for nanocrystals possessing the diameter equal to 2 nm. This value of decay time is well accorded with our interpretation on the origin of the PL attributed to Ge grains. The measured lifetime for wavelengths between 1200 and 1400 doesn't present strong dependence on wavelength.

Under the confinement effect the wave functions extend in the reciprocal space; and the probability of a direct transition without phonon increases. Niquet *et al.*[11] with *ab initio* calculation showed that for decreasing the nanocrystal size from 8 to 2 nm, the rate of non phonon assisted radiative recombination increases from 10^2 to 10^7.

A similar result was obtained in the case of silicon with nanometric size [12]. By increasing the size of nanocrystals, overlapping of the wave functions decreases, which implies to change the mechanism of recombination from direct to indirect and equally increase of the radiative lifetime; hence transition is indirect and phonon assisted with the long radiative lifetime of excited state (0.6 sec at 300 K [13]). In the case of germanium, the band structure of bulk state contains of a minimum of conduction band at Γ point with a gap equal to 0.8 eV and a minimum at point L
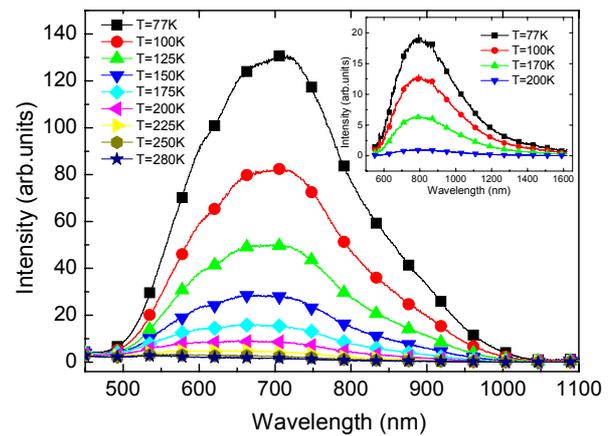
with a gap of 0.66 eV. Contrary to silicon, the difference of energy between the indirect (0.66 eV) and direct (0.8 eV) transition is weak (0.14 eV), and suggests that a direct and rapid recombination could exist in the case of germanium nanocrystals. However the effective mass of the electrons at point L is grand compared to Γ point which implies that under the confinement effect. The electronic states, corresponding to the direct transition become more energetic than indirect transition. When the size diminishes, indirect transition is more favorable energetically. According to Niquet *et al.* [11] these arguments permit to explain why the radiative lifetime of the excited state isn't as low as that obtained in the semiconductors with direct gap. Hence, the contribution of the phonon assisted transitions is so probable.

2.3. Temperature dependence
2.3.1. Continuum photoluminescence
i) Band centered at 800 nm
Temperature dependence of the intensity of visible PL corresponding to T_a=350 °C is represented in figure 3. For observing better intensity, excitation was effectuated utilizing the 313 nm ray of a UV Mercury lamp, and for comparison the sample excited by 325 nm ray of He-Cd laser is shown in the inset. The PL describes a very rapid decrease of intensity by increasing and temperature. This behavior is indicative of the non-radiative temperature activated defects which are present in the samples.

When an electron-hole pair recombines, a photon can be emitted, but another physical non-radiative process could intervene too. In fact, in the semiconductors with an indirect band gap, non-radiative transition is normally dominant process; for example, in the Si or Ge, the radiative lifetime (τ_r) is in the order of magnitude of second, however, the non-radiative lifetime τ_{nr} is, several orders of magnitude lower. Since the total recombination rate w=1/τ (in which τ is decay time) is the summation of the radiative (w_r=1/τ_r) and non-radiative (w_{nr}=1/τ_{nr}) recombination rate, it gives:
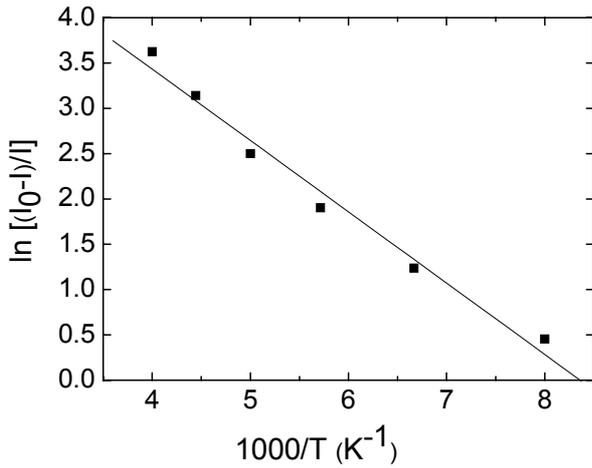
Figure 4. Evolution of $\ln[(I(77K)\text{-}I(T))/I(T)]$ versus T^{-1} for samples annealed at T_a=350 °C.

$$\frac{1}{\tau} = \frac{1}{\tau_r} + \frac{1}{\tau_{nr}}, \tag{4}$$

in which, τ is the decay time measured in the time resolved PL experiences.

The radiative performance can be written as,

$$\eta = \frac{w_r}{w} = \frac{w_r}{w_r + w_{nr}} = \frac{1/\tau_r}{1/\tau_r + 1/\tau_{nr}} = \frac{\tau_{nr}}{\tau_r + \tau_{nr}}. \tag{5}$$

There are a lot of non-radiative recombination processes, of which the most important processes are the Auger effect, phononic deexcitation, recombination through surface or deep traps (deep centers). If the multi-phonons recombination constitutes the principal mechanism, in these centers, the probability of non-radiative recombination has a strong dependence on temperature according to Arrhenius law [14],

$$w_{nr} = \frac{1}{\tau_{nr}} = C \exp\left(-\frac{E}{K_B T}\right), \tag{6}$$

in which, E is the activation energy of defects, K_B is Boltzmann constant and T is the temperature. This is because the PL intensity is proportional to radiative efficiency, (which varies as a function of temperature), according to the relation of,

$$I = A\left(1 + B\exp\left(-\frac{E}{K_B T}\right)\right)^{-1}. \tag{7}$$

At low temperature, the exponential term becomes negligible and for $I_0=A$ the intensity becomes,

$$I_{norm} = \frac{I}{I_0} = \left(1 + B\exp\left(-\frac{E}{K_B T}\right)\right)^{-1}. \tag{8}$$

Hence the activation energy is obtained by the slope of the linear curve of this function,

$$Ln\left[\frac{I_0 - I}{I}\right] = \ln B - \frac{E}{k_B T}. \tag{9}$$

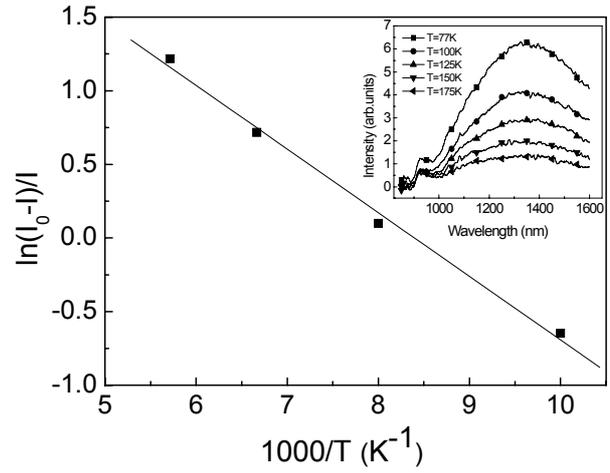Evolution of $\ln\left[\dfrac{I(77K) - I(T)}{I(T)}\right]$ as a function of T^{-1}

Figure 5. Evolution of $\ln((I(77K)\text{-}I(T))/I(T))$ versus T^{-1} for PL intensity of the sample annealed at T_a=450°C. Inset illustrates the intensity quenching of the sample.

with I the integrated intensity of luminescence at temperature T, for the sample annealed at T_a=350 °C (represented in figure 4) is linear, which is coherent with the existence of a thermally activated and non-radiative recombination phenomenon whose probability follows the Arrhenius law. The activation energy of non-radiative defects was calculated from the slope of the line equal to 68 meV.

ii) Band centered at 1350 nm

The dependence of PL as a function of the temperature is represented in figure 5 for the sample annealed at T_a=450°C; the effect of the temperature is similar to that observed for the band at 800 nm. The PL intensity at 175K decreases by factor 7 compared to that at 77 K. For higher temperature PL wasn't measurable, hence a non-radiative phenomenon steel exists in samples annealed down to 400°C. Therefore, although the radiative defects disappear due to annealing the other type of non radiative defects are present yet. The activation energy of non-radiative defects was calculated from the slope of the line equal to 37 meV.

2.3.2. Time resolved Photoluminescence

Measurement of the luminescence decay time was effectuated as a function of temperature at 1350 nm for the sample annealed at T_a=450°C. The entire time resolved curves (inset of figure 6) can be fitted by single exponential function. Evolution of decay time with temperature (represented in figure 6) is described as a decreasing function.

The luminescence decay time is a result of the contributions of radiative and non-radiative parts according to the expression,

$$\frac{1}{\tau} = \frac{1}{\tau_r} + \frac{1}{\tau_{nr}}, \tag{10}$$

in which τ, τ_r and τ_{nr} are the total (measured), radiative and non-radiative decay times, respectively. Similar to continuum PL, the contribution of non-radiative and thermally activated decay could be considered as non-
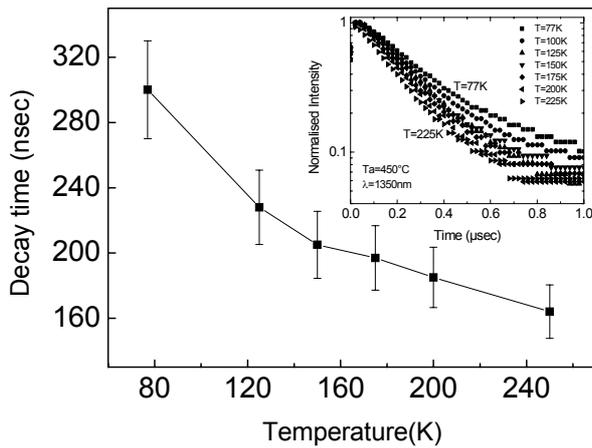
Figure 6. PL Decay of the GeO$_x$ thin film annealed at 450°C for different measurement temperatures for λ=1350 nm.

Figure 7. Evolution of $1/\tau$ as a function of the inverse of the measured temperature for the GeO$_x$ thin film annealed at 450 C. The experimental points are simulated by a decreased exponential.

radiative decay time as,

$$\frac{1}{\tau_{nr}} \propto \exp\left(-\frac{E}{K_B T}\right), \tag{11}$$

in which, E is the activation energy of defects; the measured decay time (τ) is written as,

$$\frac{1}{\tau} = \frac{1}{\tau_r} + \alpha \exp\left(-\frac{E}{K_B T}\right). \tag{12}$$

Evolution of $1/\tau$ as a function of $1/T$ for T_a=450°C (figure 7) is well described by the proposed model. According to this model, the simulation gives the activation energy of 27 meV and radiative life time (τ_r) equal to 263 ns. These values are in line with the values obtained before.

3. Summary and conclusion
Sub-stoichiometric germanium oxide thin films were prepared by electron beam evaporation technique, For T_a=350°C visible PL band centered at 800 nm was attributed to dangling band defects and for higher annealing temperatures NIR PL was attributed to confinement of excitons in Ge nanostructures. Immeasurable decay time for visible PL and 270 *ns* for NIR PL confirm our interpretation about the origin of PL at different annealing temperatures. Temperature dependence of intensity and decay time were studied; rapid intensity quenching also is coherent with our results and activation energy of non-radiative and radiative defect were measured. Time resolved PL results fitting are in conformity with our proposed model. Radiative decay time and activation energy obtained by fitting the curve are support the previous results obtained by other ways. For temperatures higher than 500°C, PL disappears, which is caused by growing of the nanostructures and loss of confinement effect.

References
1. T Shimizu-Iwayama, K Fujita, S Nakao, K Saitoh, T Fujita and N Itoh, *J. Appl. Phys.* **75** (1994) 7779.
2. S Charvet, R Madelon, F Gourbilleau and R Rizk, *J. Appl. Phys.* **85** (1999) 4032.
3. H Rinnert, M Vergnat, G Marchal and A Burneau, *Appl. Phys. Lett.* **72** (1998) 3157.
4. M Zacharias, J Bläsing, M Löhmann and J Christen, *Thin Solid Films* **278** (1996) 32.
5. M Ardyanian, H Rinnert, X Devaux and M Vergnat, *Appl. Phys. Lett.* **89** (2006) 011902.
6. L Skuja, H Hosono, M Mizuguchi, B Güttler and A Silin, *J. Lumin.* **87** (2000) 699.
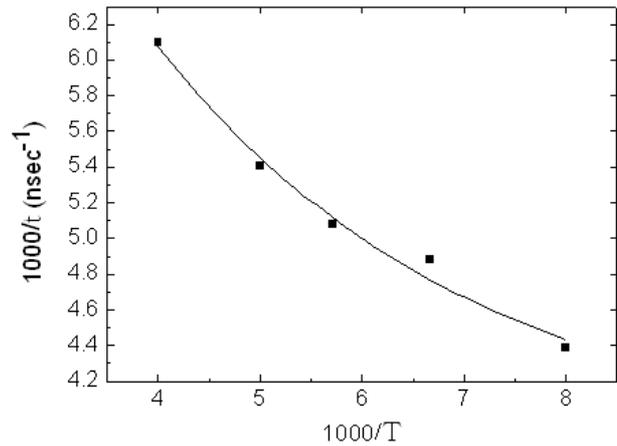7. X L Wu, T Gao, G G Siu, S Tong and X M Bao, *Appl. Phys. Lett.* **74** (1999) 2420.
8. M Ardyanian, H Rinnert and M Vergnat, *J. Lumin.* **129** (2009) 729.
9. O Jambois, H Rinnert, X Devaux and M Vergnat, *J. Appl. Phys.* **100** (2006) 123504.
10. S Takeoka, M Fujii, S Hayashi and K Yamamoto, *Phys. Rev. B* **58** (1998) 7921.
11. Y M Niquet, G Allan, C Delerue and M Lannoo, *Appl. Phys. Lett.* **77** (2000) 1182.
12. J P Proot, C Delerue and G Allan, *Appl. Phys. Lett.* **61** (1992) 1948.
13. B Mombelli, in *Processus optiques dans les solides*, Masson, Paris (1995) pp. 26.
14. S Shionoya, in *"Luminescence of Solids"*, edited by D R Vij, Plenum Press, New York (1998) 95.